Deoxygenation and Desulfurization of Oxiranes and Thiiranes by Carbenes: A Theoretical Study

Ming-Der Su*[a] and San-Yan Chu*[b]

Abstract: The potential-energy surfaces for the abstraction reactions of carbenes with oxirane and thiirane have been characterized in detail by using density functional theory (B3LYP/6-31G*), which include zero-point corrections. Six carbene species: dimethylcarbene, cyclobutylidene, cyclohexylidene, phenylchlorocarbene, methoxyphenylcarbene, and dimethoxycarbene have been chosen in this work as model reactants. All the interactions involve the initial formation of a loose donor–acceptor complex followed by a heteroatom shift via a two-center transition state. The complexation energies, activation barriers, and enthalpies of the reactions were used comparatively to determine the relative carbenic reactivity, as well as the influence of substituents on the reaction potential-energy surface. As a result, our theoretical investigations indicate that, irrespective of deoxygenation and desulfurization, the relative carbenic reactivity decreases in the order: cyclobutylidene > dimethylcarbene ≈ cyclohexylidene > phenylchlorocarbene > methoxyphenylcarbene ≫ dimethoxycarbene. Namely, the alkyl-substituted carbene abstractions are much more favorable than those of the π-donor-substituted carbenes. Moreover, for a given carbene, while both deoxygenation and desulfurization are facile processes, the deoxygenation reaction is more exothermic but less kinetically favorable. Furthermore, a configuration-mixing model based on the work of Pross and Shaik is used to rationalize the computational results. The results obtained are in good agreement with available experimental observations, and allow a number of predictions to be made.

Keywords: carbenes · density functional calculations · oxiranes · thiiranes

Introduction

Reductive deoxygenation of organic molecules has been a topic of considerable interest over the past three decades, from mechanistic as well as synthetic perspectives.[1] A varied series of reagents has been used for the purpose of organic synthesis and of proving structures,[2] illustrating its richness and complexity. Basically, deoxygenation reactions can be classified into two principal types: a) those in which oxygen is simply abstracted from a molecule and b) those in which oxygen removal occurs in tandem with intermolecular coupling. The former is best exemplified by the deoxygenation of oxiranes (ethylene oxides and epoxides[1a]) to give alkenes [Eq. (1)].[3] The most common example of the second mode of
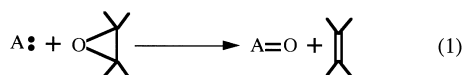
deoxygenation is the reductive coupling of ketones and aldehydes to yield olefins [Eq. (2)].[4] Nevertheless, the detailed reaction mechanism of deoxygenation has not been firmly established by either experimental or theoretical studies, and many key questions remain open.

$$A\colon\colon + \quad \longrightarrow \quad A \quad \longrightarrow \quad A\mathord{=}\!\!\!\!{O} + \quad \quad (2)$$
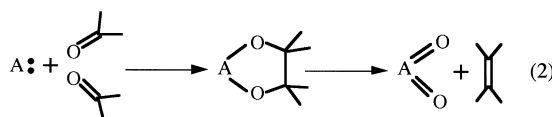
Similarly, sulfur-containing compounds have played an increasingly important role in organic synthesis owing to the ease of sulfur incorporation into complex structures and the ease of its removal as required by the synthesis. It is therefore not surprising that reductive desulfurization of organic molecules has been subjected to extensive synthetic and mechanistic investigations.[5] In fact, the search for general and selective methods of desulfurization has led to the development of many procedures and reagents.[6] Desulfurization appears to be a general process, the chemistry of which parallels that of deoxygenation. In connection with studies of oxygen-transfer reactions, it is therefore desirable to examine the reaction mechanisms of sulfur atom abstractions in relation to the analogous reactions of heteroatom-transfer chemistry.

$$A\colon\colon + \quad O \quad \longrightarrow \quad A\mathord{=}\!O + \quad \quad (1)$$

[a] Prof. M.-D. Su
School of Chemistry
Kaoshiung Medical University
Kaoshiung 80708, Taiwan (Republic of China)

[b] Prof. S.-Y. Chu
Department of Chemistry, National Tsing Hua University
Hsinchu 30043, Taiwan (Republic of China)
Fax: (+886) 35-711082
E-mail: ggs@chu1.chem.nthu.edu.tw

Recently, through the elegant studies performed by Lusztyk, Warkentin, and many others,[7, 8] it was found that singlet carbenes are capable of abstracting oxygen and sulfur atoms from oxiranes and thiiranes, respectively, undergoing the reaction shown above [Eq. (1)]. Several qualitative conclusions concerning the oxirane deoxygenation and thiirane desulfurization can be made: a) the magnitudes of the rate constants for heteroatom transfer are dependent on the philicity of the carbene intermediate; b) trends in the kinetic data suggest that oxygen and sulfur transfer occur by concerted mechanisms through ylide-like transition states; c) ylides formed by the attack of carbenes on heteroatom donors were not observed for any of the heteroatom-transfer reactions; and d) absolute rate constants for the heteroatom transfers show that both deoxygenation and desulfurization are facile processes, the latter proceeding much faster than the former.

No estimates of the absolute activation energies of such abstractions are, to our knowledge, available yet from experiments.[9] In fact, it is very difficult to detect the intermediate as well as the transition state due to limitations in current experimental techniques. For a long time chemists have used transition-state structures to explain the transformation of reactants into products. Correct evaluations of transition-state geometries and energies are a powerful approach to the study of chemical reaction mechanisms. In this regard, in order to examine the mechanisms of the heteroatom-transfer reactions, we have undertaken a systematic investigation of the abstraction reactions of various carbene species [Eq. (3)] by using density functional theory (DFT).

$$\text{>C:}(1-6) + \underset{\triangle}{\overset{X}{\triangle}} \xrightarrow{(X = O,S)} \text{>C=X} + \text{>—<} \qquad (3)$$
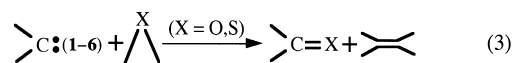
Abstract in Chinese: 以密度函數計算方法 (B3LYP/6-31G*)含零點振動校正來探討碳烯基和環氧乙烷及環硫乙烷進行抓取異原子反應的位能面。六種碳烯基含二甲基碳烯基(1)，環丁烷碳烯基(2)，環己烷碳烯基(3)，苯、氯碳烯基(4)，甲氧、苯碳烯基(5)，雙甲氧碳烯基(6)選做為此工作反應物的模型分子。碳烯基先和環乙烷形成弱作用複合物，再進入異原子轉移的過渡態。我們以複合物能量，反應能障及反應熱以判定各碳基的反應活性，及取代基對反應位能面的影響。計算結果顯示對二種環乙烷，六種碳烯基活性順序為 2>1～3>4>5>6，即含烷類取代基的碳烯基活性高於含 π 電子給予者取代基的碳烯基。對於同一碳烯基而言，抓氧及抓硫均為容易進行反應。但抓氧反應放熱較多，而且活化能較高。最後我們以 Pross 及 Shaik 的電子組態模型來詮釋計算結果，理論計算相當吻合實驗結果，也可以進一步做一些預測。

Six carbenes (1 – 6), which mimic the experimental work,[7] have been chosen as model systems for heteroatom transfer in this work. These carbene species are dimethylcarbene (1), cyclobutylidene (2), cyclohexylidene (3), phenylchlorocarbene (4), methoxyphenylcarbene (5), and dimethoxycarbene (6). We compared both the deoxygenation of oxiranes and the desulfurization of thiiranes (ethylene sulfides[5a]) by the same carbene species. Our approach was to calculate a number of examples of the reaction for which activation parameters are available, as is the case for carbenes 1 – 6. Even if the uncertainties in the calculated activation parameters for individual reactions are too large for definite conclusions to be drawn, the relative values for a number of related reactions are likely to be reproduced, at least qualitatively. Comparison of the predicted pattern of rates with experiment should then provide a more reliable test of the predicted mechanism than any calculation for a single case.

The purpose of the present DFT mechanical study was to locate the transition state for the reaction given in Equation (3), to carry out a vibrational analysis at this stationary point, and to explain why there appears to be a barrier for the carbene abstractions. Through the study, we may then clarify the factors that affect the relative stability of intermediates and control the activation barriers for these abstraction reactions. The other impetus for this work was an attempt to ascertain whether such abstractions occur in a concerted fashion or in a stepwise biradical manner with a highly distorted transition state. Besides these, our aim was further to search for a general theory of reactivity for such abstraction reactions, and to decide whether reactivity can be predicted through an understanding of the reaction mechanisms, although qualitative in nature, from either simple molecular-orbital or valence-bond considerations. Furthermore, an understanding of the factors that can facilitate both the oxirane deoxygenation and thiirane desulfurization may suggest further synthetic applications.

The results are divided into three major parts. First, the results for both the oxirane deoxygenation and thiirane desulfurization. Second, the comparison between deoxygenation and desulfurization.. In the last section, the origin of the barrier heights and reaction enthalpies for these abstraction reactions is discussed.

Computational Methods

All geometries were fully optimized without imposing any symmetry constraints, although in some instances the resulting structure showed various elements of symmetry. For our DFT calculations, we used the hybrid gradient-corrected exchange functional proposed by Becke,[10] combined with the gradient-corrected correlation functional of Lee, Yang, and Parr.[11] This functional is commonly known as B3LYP, the results of which have been shown to be closer to the QCISD(T) reference than the MP2 value.[12] For C, H, O, and S the standardized 6-31G* basis set was used.[13] We thus denote our B3LYP calculations by B3LYP/6-31G*. The spin-unrestricted (UB3LYP) formalism used for the open-shell (triplet) species, and their $\langle S^2 \rangle$ values were all nearly equal to the ideal value (2.00). The vibrational frequencies were investigated to characterize the structures as minima or transition states. Relative energies are corrected for vibrational zero-point energies (ZPE, not scaled). All calculations were performed with the GAUSSIAN 94/DFT package.[14]

Results and Discussion

Structures and energies of intermediates and transition states

Carbene and oxirane: Before discussing the geometrical optimizations and the potential-energy surfaces for the abstraction reactions, it is perhaps worthwhile to recall briefly the electronic structure of a carbene. It is well established that carbene has a relatively low-lying σ lone-pair orbital and a higher lying π (p in C) orbital.[15] There are two low-lying states, singlet and triplet, depending on whether the electronic configuration is $\sigma^2\pi^0$ (singlet) or high spin $\sigma^1\pi^1$ (triplet). The optimized reactant geometries of dimethylcarbene (**1**), cyclobutylidene (**2**), cyclohexylidene (**3**), phenylchlorocarbene (**4**), methoxyphenylcarbene (**5**), and dimethoxycarbene (**6**) for each reaction obtained at the B3LYP/6-31G* level of theory are presented in in Figures 1–6, respectively. The triplet structures of carbenes **1–6** were also optimized (UB3LYP/6-31G*) and their geometrical parameters are shown in parentheses.[16] Calculated values for the energy difference
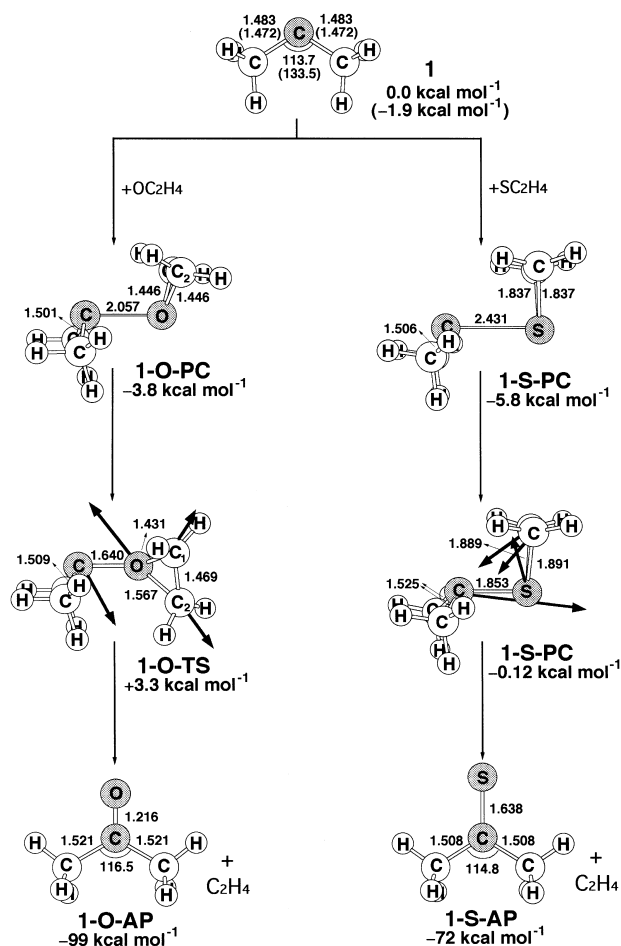

Figure 1. The optimized geometries (bond lengths in Å and angles in degrees) for the precursor complexes (PC), transition states (TS), and abstraction products (AP) of oxirane and thiirane with dimethylcarbene (**1**). All were calculated at the B3LYP/6-31G* level of theory. Values in parentheses are in the triplet state. The relative energies are taken from Tables 1 and 3. The heavy arrows indicate the main atomic motions in the transition-state eigenvector.
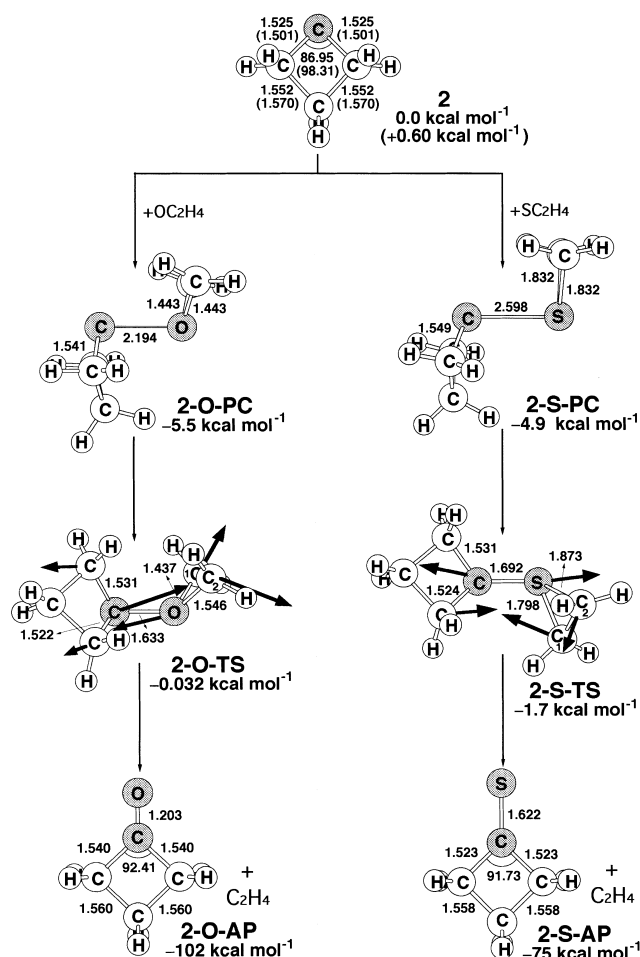

Figure 2. The optimized geometries (bond lengths in Å and angles in degrees) for the precursor complexes (PC), transition states (TS), and abstraction products (AP) of oxirane and thiirane with cyclobutylidene (**2**). All were calculated at the B3LYP/6-31G* level of theory. Values in parentheses are in the triplet state. The relative energies are taken from Tables 1 and 3. The heavy arrows indicate the main atomic motions in the transition-state eigenvector.

ΔE_{st} (= $E_{triplet} - E_{singlet}$) between the singlet and triplet states of various carbenes (ABC:) are given in Table 1; a negative value for ΔE_{st} implies that the triplet is predicted to be the ground state rather than the singlet.

Dimethylcarbene (**1**) is now believed to have a singlet ground state with a small ΔE_{st} of 1.0–1.5 kcal mol^{-1}.[17] However, our B3LYP/6-31G* calculations predict that the singlet state of this carbene is no more than 1.9 kcal mol^{-1} above the triplet ground state. In any event, these calculational results strongly imply that the energy separation between the singlet and triplet states of dimethylcarbene is very small. In fact, it has been understood for some time on a theoretical level that there are two distinct ways to control the singlet–triplet gap.[18] The first is through a change in geometry, primarily the bond angle (ϕ) at the carbene center.[19, 20] Theory predicts that as ϕ contracts, the energy of the singlet carbene decreases relative to that of the triplet. Our B3LYP/6-31G* results confirm this prediction. For example, cyclobutylidene (**2**, $\phi = 87°$) is found to have a singlet ground state with ΔE_{st} of 0.60 kcal mol^{-1}, whereas
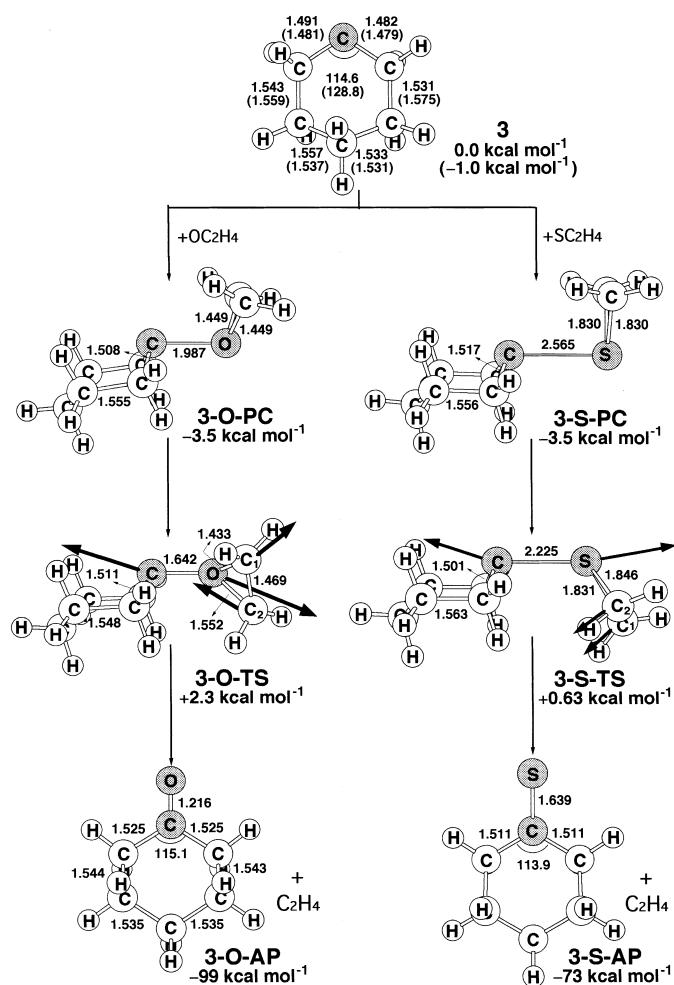
Figure 3. The optimized geometries (bond lengths in Å and angles in degrees) for the precursor complexes (PC), transition states (TS), and abstraction products (AP) of oxirane and thiirane with cyclohexylidene (**3**). All were calculated at the B3LYP/6-31G* level of theory. Values in parentheses are in the triplet state. The relative energies are taken from Tables 1 and 3. The heavy arrows indicate the main atomic motions in the transition-state eigenvector.
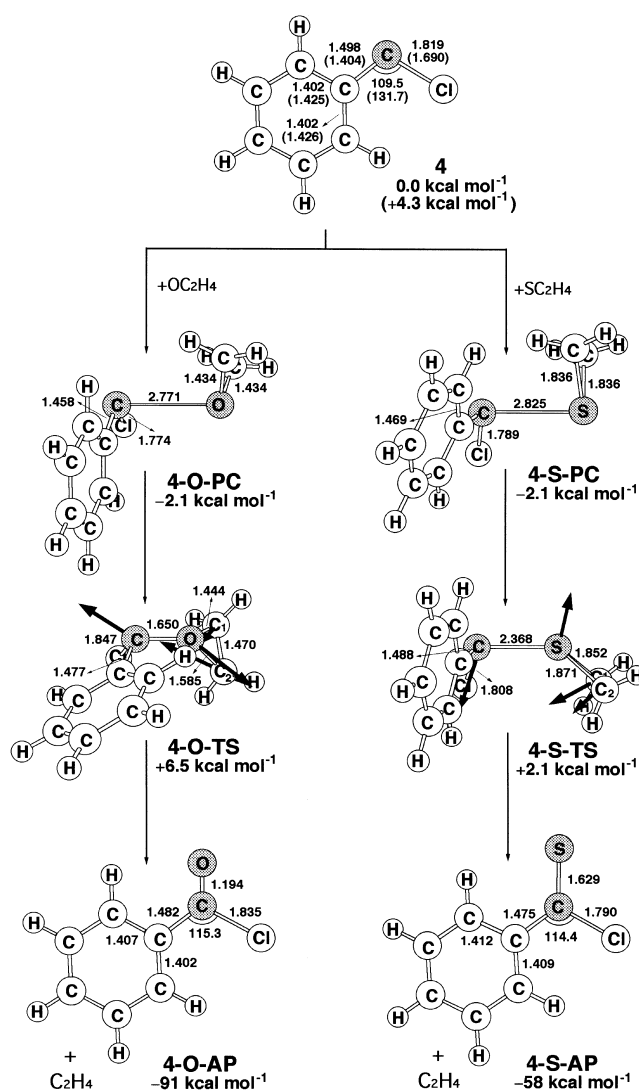
Figure 4. The optimized geometries (bond lengths in Å and angles in degrees) for the precursor complexes (PC), transition states (TS), and abstraction products (AP) of oxirane and thiirane with phenylchlorocarbene (**4**). All were calculated at the B3LYP/6-31G* level of theory. Values in parentheses are in the triplet state. The relative energies are taken from Tables 1 and 3. The heavy arrows indicate the main atomic motions in the transition-state eigenvector.

cyclohexylidene (**3**, $\phi = 115°$) possesses a triplet ground state with ΔE_{st} of -1.0 kcal mol^{-1}.[12] The second factor that affects the relative energy between the singlet and triplet states is related to electronic perturbation, which depends on the nature of substituents.[21] It is generally accepted that the singlet state appears to be the ground state of an acyclic carbene ABC: whenever either A or B has a lone-pair π-donor atom bonded directly to the carbene center.[22] Again, our theoretical calculations are in good accord with this conclusion. For instance, the ground state of C(C$_6$H$_5$)(Cl) (**4**), C(C$_6$H$_5$)(OCH$_3$) (**5**), and C(OCH$_3$)$_2$ (**6**) is predicted to be the singlet with ΔE_{st} of 4.3, 19, and 54[23] kcal mol^{-1}, respectively, based on the B3LYP/6-31G* level of theory.

We now turn to the computed structures reported in Figures 1–6. It is understood and widely accepted that the triplet carbene (ABC:) has a significantly wider bond angle ϕ and shorter bond lengths (C–A and C–B) than the closed-shell singlet state.[20–22] There are, however, two exceptions found in Figures 5 and 6, in which the optimum C–O bond lengths in both triplet C(OCH$_3$)$_2$ and triplet C(C$_6$H$_5$)(OCH$_3$)

are longer than those in the singlet state.[24] The reason for this is presumably the fact that conjugation of the triplet carbene π electron to the two π electrons of the OCH$_3$ group is less important than the delocalization of the latter into the empty p-π orbital on the carbene carbon atom in the singlet state.

The optimized geometries of the calculated compounds oxirane and thiirane at the B3LYP/6-31G* level are collected in Table 2. As one can see in Table 2, the agreement for both bond lengths and bond angles in the compounds between the B3LYP results and experiments[25] is quite good, with the bond lengths and angles in agreement to within 0.023 Å and 1.7°, respectively. It is therefore believed that the B3LYP calculations provide an adequate theoretical level for further investigations of molecular geometries, electronic structures, and kinetic features of the reactions.

Furthermore, there is general agreement that the abstraction reactions of carbenes proceed via the singlet state,[26] and
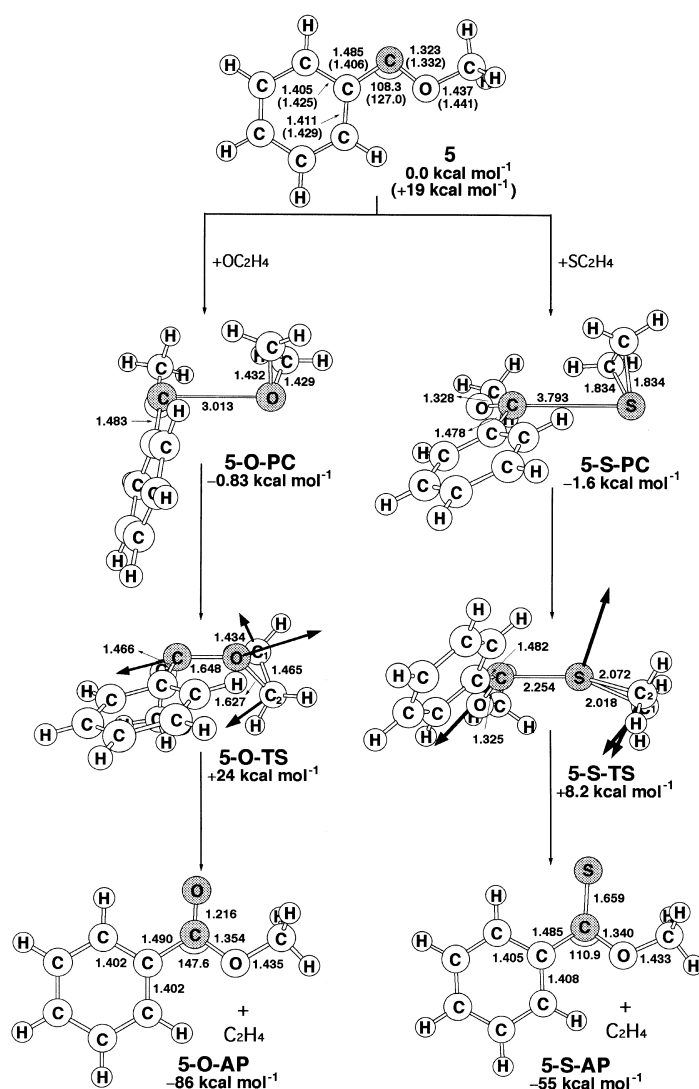
Figure 5. The optimized geometries (bond lengths in Å and angles in degrees) for the precursor complexes (PC), transition states (TS), and abstraction products (AP) of oxirane and thiirane with methoxyphenyl-carbene (**5**). All were calculated at the B3LYP/6-31G* level of theory. Values in parentheses are in the triplet state. The relative energies are taken from Tables 1 and 3. The heavy arrows indicate the main atomic motions in the transition-state eigenvector.
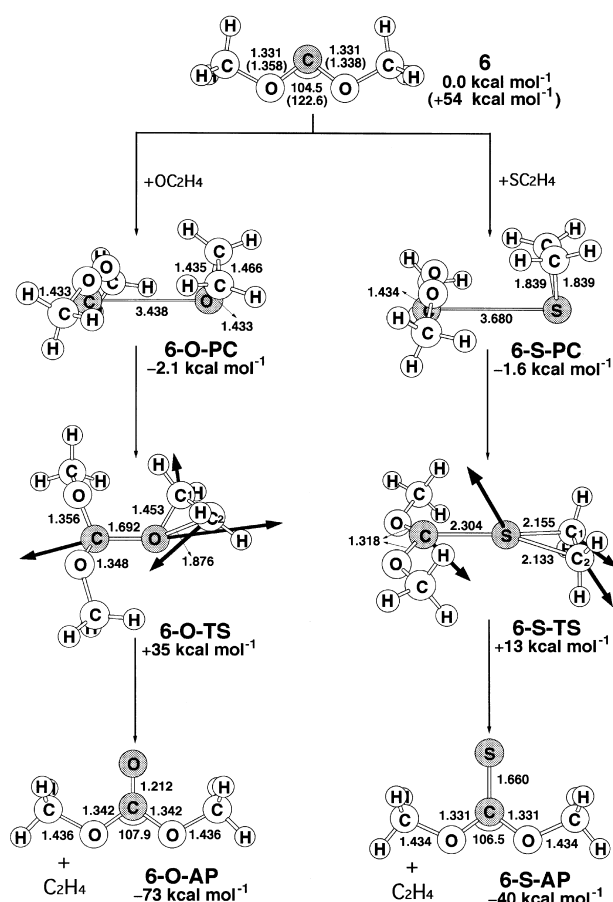

Figure 6. The optimized geometries (bond lengths in Å and angles in degrees) for the precursor complexes (PC), transition states (TS), and abstraction products (AP) of oxirane and thiirane with dimethoxycarbene (**6**). All were calculated at the B3LYP/6-31G* level of theory. Values in parentheses are in the triplet state. The relative energies are taken from Tables 1 and 3. The heavy arrows indicate the main atomic motions in the transition-state eigenvector.

Table 1. Relative energies for singlet and triplet carbenes and for the process carbene + oxirane → precursor complex → transition state → abstraction products.[a,b]

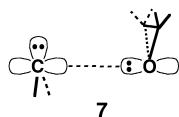| System	ΔE_{st}[c] [kcal mol^{-1}]	ΔE_{cpx}[d] [kcal mol^{-1}]	$\Delta E^{\neq}$[e] [kcal mol^{-1}]	ΔH[f] [kcal mol^{-1}]
1 H₃C CH₃	− 2.276 (− 1.879)	− 6.318 (− 3.780)	+ 0.9259 (+3.316)	− 99.67 (−98.60)
2	− 0.4746 (+0.6037)	− 8.913 (− 5.462)	− 3.758 (− 0.0320)	− 104.3 (− 102.3)
3	− 3.125 (− 1.027)	− 8.244 (− 3.478)	− 1.921 (+2.321)	− 102.1 (− 99.01)
4 Ph Cl	+ 4.563 (+ 4.291)	− 2.885 (− 2.093)	+ 5.515 (+ 6.462)	− 90.82 (− 90.88)
5 Ph OCH₃	+ 19. 90 (+19.23)	− 1.415 (− 0.8289)	+ 24.32 (+24.40)	− 86.39 (−86.28)
6 CH₃O OCH₃	+ 54.64 (+ 53.55)	− 2.824 (− 2.115)	+ 34.87 (+34.55)	− 72.86 (−72.75)

[a] At the B3LYP/6-31G* level. The B3LYP optimized structures of the stationary points see Figures 1 – 6. [b] Energies differences in parentheses have been zero-point corrected. [c] Energy relative to the corresponding singlet state. A positive value means the singlet is the ground-state. [d] The stabilization energy of the precursor complex, relative to the corresponding reactants. [e] The activation energy of the transition state, relative to the corresponding reactants. [f] The exothermicity of the product, relative to the corresponding reactants.

much of the experimental work on carbenes (such as **1 – 6**) involves initial generation of the singlet from the appropriate precursor.[7, 8] Indeed, this is consistent with results based on spin conservation, which predict that a singlet carbene is required to produce singlet abstraction products.[27] Additionally, as noted earlier, all of the carbenes **1 – 6** considered in this study have either a singlet ground state or a triplet ground state with a relatively small singlet–triplet energy gap. Hence, our investigation will be confined to the singlet surfaces.

Let us now explore the potential-energy surface for these abstraction reactions. When we searched the potential-energy surface for transition structures of the deoxygenation of oxiranes producing a ketone and an alkene, we noticed an initial decrease in total energy as compared with the isolated molecules at large separation. Indeed, it is reasonable to expect that the reaction between carbene and oxirane occurs

Table 2. Comparison of structures of oxirane and thiirane.[a–c]

	O △	S △
C−X	1.429, (1.428)	1.838, (1.815)
C−C	1.462, (1.469)	1.481, (1.484)
C−H	1.090, (1.086)	1.087, (1.083)
C-X-C	61.80, (61.62)	48.27, (47.51)
H-C-H	115.2, (116.9)	115.8, (114.5)

[a] At the B3LYP/6-31G* level. [b] Values in parentheses denote the experimental data. For oxirane and thiirane see ref. [24a] and [4b], respectively. [c] Bond lengths are in Å and bond angles are in degrees.

with the initial formation of a precursor complex (PC), in which the vacant p-π orbital on the carbene is oriented for maximum interaction with the σ lone pair on the oxygen. Therefore, as shown in Figures 1–6, the deoxygenation of oxirane by carbenes initiates the formation of a two-center ylide-like complex (**1-O-PC**, **2-O-PC**, **3-O-PC**, **4-O-PC**, **5-O-PC**, and **6-O-PC**) with optimal overlap between the carbene carbon and oxygen atoms through a parallel plane approach of the two molecules (see structure **7** in Scheme 1). We note that the calculated Hessian matrices had no negative eigenvalues, confirming their identification as true minima on the potential-energy surface. In fact, it is well-known[28] that the interaction between the empty p orbital on the abstracting species (carbene) and the lone-pair orbital on a Lewis base (oxirane) can cause lone-pair donation that stabilizes the intermediate complex (donor–acceptor complex) initially formed in the abstraction reaction (see Scheme 1).

Scheme 1.

Complexation energies computed for the formation of these intermediate complexes are given in Table 1. The DFT results of Figures 1–6 show that the calculated C−O bond lengths between the carbene and the oxirane in the precursor complexes **1-O-PC**, **2-O-PC**, and **3-O-PC** are 2.06 Å, 2.19 Å, and 1.99 Å, respectively, whereas **4-O-PC**, **5-O-PC**, and **6-O-PC** have a C−O distance of 2.77 Å, 3.01 Å, and 3.44 Å, respectively. We attribute the weak intermediate bond and long C−O distance in the last three precursor complexes to the steric effect of bulky substituents on the carbene species. Coincidentally, it is of interest to stress that a longer C−O distance should correlate with a smaller value for the intermediate stabilization energy. For instance, as shown in Table 1, of the investigated species the complexation energies of **1-O-PC**, **2-O-PC**, and **3-O-PC** are estimated to be 3.8, 5.5, and 3.5 kcal mol^{-1} at the B3LYP/6-31G* level, respectively, which are larger than those for **4-O-PC** (2.1 kcal mol^{-1}), **5-O-PC** (0.83 kcal mol^{-1}), and **6-O-PC** (2.1 kcal mol^{-1}). Note that, even when the ZPE correction is considered, the stabilization energies of these precursor complexes relative to their corresponding reactants are still less than 6.0 kcal mol^{-1}. Our attempt to determine the molecular complexes at much shorter C−O distance for the addition of carbene to oxirane were not successful. Thus, the present calculations indicate

that those precursor complexes obtained in this work can be referred to as rather loose donor–acceptor complexes. In other words, our theoretical findings suggest that the ylide-like precursor complex exists only as a shallow minimum and experimental detection of such an intermediate formed during the reaction is not possible. Our model prediction is consistent with experimental observations, in which ylides from the reaction of carbenes with oxiranes were not detected by laser flash photolysis (LFP) methods.[7, 8]

In addition, it should be noted that charge transfer between oxirane and carbene occurs despite their large separation. This charge separation may be used as a guide to examine the carbene philicity. For instance, the B3LYP results show that the net charge-transfer decreases in the order: **3-O-PC** (0.130 au) > **1-O-PC** (0.113 au) > **2-O-PC** (0.0822 au) > **5-O-PC** (0.0166 au) > **4-O-PC** (0.0142 au) > **6-O-PC** (0.0119 au). This suggests that the carbenes **1**, **2**, and **3** are electron-deficient (electrophilic) molecules, the carbenes **4** and **5** are ambiphilic in nature, and carbene **6** is considered to be nucleophilic in character. These features are in reasonable agreement with the previous study[7] based on Moss' carbene philicity scale.[27]

We then examined the transition state for the oxygen transfer from oxirane to carbene [Eq. (1)]. The transition-state structures (**1-O-TS**, **2-O-TS**, **3-O-TS**, **4-O-TS**, **5-O-TS** and **6-O-TS**) obtained for the abstraction reaction are displayed in Figures 1–6, respectively. All the transition states at the B3LYP level of theory were confirmed by the calculation of the energy Hessian, which shows only one imaginary vibrational frequency: 455i cm^{-1} (**1-O-TS**), 379i cm^{-1} (**2-O-TS**), 385i cm^{-1} (**3-O-TS**), 380i cm^{-1} (**4-O-TS**), 595i cm^{-1} (**5-O-TS**), and 658i cm^{-1} (**6-O-TS**). The arrows in Figures 1–6 illustrate the directions in which the atoms move in the normal coordinate corresponding to the imaginary frequency. The transition vector (normal mode associated with the imaginary frequency) consists mainly of the forming C−O stretching mode coupled to O−C bond breaking in the oxirane and is compatible with the changes in geometry that occur during the reaction. Apparently, the transition states connect the corresponding precursor complexes to the abstraction products. It should be emphasized that the primary similarity among these transition states is the two-center pattern involving carbon (carbene) and oxygen (oxirane). Moreover, the B3LYP calculations show that the forming C−O bond in the **1-O-TS**, **2-O-TS**, **3-O-TS**, **4-O-TS**, **5-O-TS**, and **6-O-TS** structures is shorter by 20%, 26%, 17%, 36%, 45%, and 51%, respectively, than the corresponding precursor complex. These structural features reveal that the three transition structures **1-O-TS**, **2-O-TS**, and **3-O-TS** take on more reactant-like character than those of **4-O-TS**, **5-O-TS**, and **6-O-TS**. As will be demonstrated below, this is consistent with the Hammond postulate,[27] which associates an earlier transition state with a smaller barrier and a more exothermic reaction.

Furthermore, the most dramatic result in our DFT calculations is that all the transition states for the oxygen-transfer reactions are asynchronous. That is, bond breaking at the C_2 carbon is far more advanced that at the C_1 carbon, but there is nonetheless some bond breaking there as well. As can be seen

in Figures 1–6, in each case one of the breaking bonds (O–C$_1$) is only slightly longer than in a normal O–C single bond of oxirane (i.e., **1-O-TS** 1.431 Å; **2-O-TS**, 1.437 Å; **3-O-TS**, 1.433 Å; **4-O-TS**, 1.444 Å; **5-O-TS**, 1.434 Å; and **6-O-TS**, 1.453 Å), while the other (O–C$_2$) is greatly stretched (i.e., **1-O-TS**, 1.567 Å; **2-O-TS**, 1.546 Å; **3-O-TS**, 1.552 Å; **4-O-TS**, 1.585 Å; **5-O-TS**, 1.627 Å; and **6-O-TS**, 1.876 Å). Notably, it is clear from these results that **6-O-TS** has the highest activation barrier structure with the most pronounced asynchronicity, while **2-O-TS** has the lowest barrier energy and is more synchronous. In principal, it is believed that the steric effect (caused by bulky substituents on the carbene and/or oxirane molecules) should enhance the asynchronicity. Despite the dramatic asynchronicity in these transition structures, the present calculations indicate that the oxirane deoxygenation reaction is still concerted, since no energy minimum corresponding to an intermediate between the transition state and products has been found. Additional support for such a concerted process comes from the work of Schuster,[8e] where the oxirane deoxygenation was found to take place with complete retention of stereochemical integrity in the alkene.
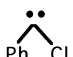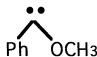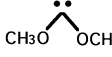
To better estimate the reactivities of carbenes **1–6** in oxygen-transfer reactions, the activation barriers were evaluated. The activation energies for the transition states **1-O-TS**, **2-O-TS**, **3-O-TS**, **4-O-TS**, **5-O-TS**, and **6-O-TS** are also summarized in Table 1. As one can see in Table 1, the energy of the transition state relative to its corresponding reactants increases in the order: **2-O-TS** (− 0.032 kcal mol^{-1}) < **3-O-TS** (2.3 kcal mol^{-1}) < **1-O-TS** (3.3 kcal mol^{-1}) < **4-O-TS** (6.5 kcal mol^{-1}) < **5-O-TS** (24 kcal mol^{-1}) < **6-O-TS** (35 kcal mol^{-1}). As a result, the dimethoxycarbene (**6**) deoxygenation should be comparatively difficult to carry out experimentally due to its highest activation barrier (estimated 35 kcal mol^{-1}), but other carbene-abstraction reactions [especially for dimethylcarbene (**1**), cyclobutylidene (**2**), and cyclohexylidene (**3**)] may readily undergo oxygen-transfer reaction in a concerted fashion. It is of importance to note that these theoretical trends are precisely what is observed by experiment;[7] this implies that the B3LYP calculations can provide a reliable theoretical level for further investigations of heteroatom-transfer reactions.

Finally, as expected, the abstraction products (AP) of the deoxygenation of oxirane by carbenes are ketones (**1-O-AP**, **2-O-AP**, **3-O-AP**, **4-O-AP**, **5-O-AP**, and **6-O-AP**) and an ethylene. The optimized product geometries and their relative energies for each abstraction reaction are also collected in Figures 1–6 and Table 1, respectively. It is worth noting that the newly formed C–O bonds in the transition structures are stretched by an average 38% relative to their final equilibrium values in absraction reactions for carbenes **1–3**, and 35% for carbenes **4–6**. Again, these structural features indicate that the alkyl-substituted carbene-abstraction reaction reaches the TS relatively early, whereas the π-donor-substituted carbene abstraction arrives at the TS relatively late. According to the Hammond's postulate,[28] one may then anticipate a larger exothermicity for the former than for the latter. This is demonstrated perfectly by evaluating the reaction enthalpies for these carbene-abstraction reactions. For instance, as seen in Table 1, the oxygen-transfer reaction is

exothermic and the exothermicity increases in the order: cyclobutylidene (**2**, − 102 kcal mol^{-1}) < cyclohexylidene (**3**, − 99.0 kcal mol^{-1}) < dimethylcarbene (**1**, − 98.6 mol^{-1}) < phenylchlorocarbene (**4**, − 90.9 kcal mol^{-1}) < methoxyphenylcarbene (**5**, − 86.3 kcal mol^{-1}) < dimethoxycarbene (**6**, − 72.8 kcal mol^{-1}). Namely, our model calculations demonstrate that the alkyl-substituted carbene abstractions are favored thermodynamically over the π-donor-substituted carbene ones.

Carbene and thiirane: Next we consider the reaction for sulfur transfer from thiirane to carbene, leading to thiones and an ethylene. In principle, the computational results of the thiirane desulfurization are similar to those noted above for the oxirane system. Namely, these exothermic reactions proceed via initial formation of a donor–acceptor complex and subsequent rearrangement through a two-center transition state to yield the eventual abstraction products. The fully optimized geometries of the reactants, precursor complexes, transition states, and products for various model reactions calculated at the B3LYP/6-31G* level are given in Figures 1–6. The energy parameters at the same level of theory are summarized in Table 3.

Table 3. Relative energies for singlet and triplet carbenes and for the process carbene + thiirane → precursor complex → transition state → abstraction products.[a,b]

System	ΔE_{st}[c] [kcal mol^{-1}]	ΔE_{cpx}[d] [kcal mol^{-1}]	$\Delta E^{\neq}$[e] [kcal mol^{-1}]	ΔH[f] [kcal mol^{-1}]
1 H$_3$C CH$_3$	− 2.276 (− 1.879)	− 7.901 (− 5.821)	− 1.245 (− 0.1186)	− 72.82 (− 71.59)
2	− 0.4746 (+ 0.6037)	− 5.980 (− 4.872)	− 2.496 (− 1.672)	− 76.34 (− 75.29)
3	− 3.125 (− 1.027)	− 5.201 (− 3.474)	− 3.096 (+ 0.6344)	− 76.36 (− 73.01)
4 Ph Cl	+ 4.563 (+ 4.291)	− 2.852 (− 2.144)	+ 0.5802 (+ 2.073)	− 57.40 (− 57.67)
5 Ph OCH$_3$	+ 19.90 (+ 19.23)	− 2.247 (− 1.630)	+ 8.300 (+ 8.230)	− 54.64 (− 54.64)
6 CH$_3$O OCH$_3$	+ 54.64 (+ 53.55)	− 2.293 (− 1.647)	+ 13.16 (+ 13.11)	− 40.43 (− 40.39)

[a] At the B3LYP/6-31G* level. The B3LYP optimized structures of the stationary points see Figures 1–6. [b] Energies differences in parentheses have been zero-point corrected. [c] Energy relative to the corresponding singlet state. A positive value means the singlet is the ground state. [d] The stabilization energy of the precursor complex, relative to the corresponding reactants. [e] The activation energy of the transition state, relative to the corresponding reactants. [f] The exothermicity of the product, relative to the corresponding reactants.

Like the oxirane deoxygenation discussed earlier, the ylide-like precursor complexes **1-S-PC**, **2-S-PC**, **3-S-PC**, **4-S-PC**, **5-S-PC**, and **6-S-PC** for thiirane desulfurization were also located at the DFT level. These adducts were confirmed to have no imaginary frequency; this indicates that they are true minima on the potential-energy surfaces. As noted previously, these intermediates correspond to donor–acceptor complexes that are stabilized by the donative interaction between lone pair electrons on the sulfur atom and a vacant p-π orbital on the carbene as illustrated in Scheme 1. However, our

B3LYP calculations indicate that they all have very long C−S distances (2.43 Å – 3.79 Å) compared with those in their corresponding abstraction products. Such long C−S distances between carbene and thiirane are also reflected in their calculated binding energies. For instance, as presented in Table 3, the energy of the precursor complex relative to its corresponding reactants is less than 4.0 kcal mol^{-1}. Consequently, it appears unlikely that the ylide-like intermediate complexes can be isolated experimentally at room temperature because their stabilization energies are too low. Our computational findings agree well with the experimental evidence. It was reported that the sulfur ylide intermediate formed during the reaction has not been observed directly by LFP.[7]

Likewise, the intermediate complex is transformed via a two-center-like transition state to the product thione and ethylene. Transition-state geometries (**1-S-TS**, **2-S-TS**, **3-S-TS**, **4-S-TS**, **5-S-TS** and **6-S-TS**) were located with full optimization and in each case were characterized by having only one imaginary vibrational frequency. As illustrated by the transition vectors in Figures 1-6, movement of the transferring sulfur atom dominates as the C=S bond forms and the two S−C bonds break. It is of interest to note that the overall feature of the structural changes in the thiirane desulfurization is essentially the same as that calculated previously in the oxirane deoxygenation. The most striking difference, however, is that almost equal separations for the two breaking S−C bonds are found in the transition structures of dimethylcarbene (**1-S-TS**), cyclohexylidene (**3-S-TS**), phenylchlorocarbene (**4-S-TS**), methoxyphenylcarbene (**5-S-TS**) and dimethoxycarbene (**6-S-TS**), which demonstrates a synchronous concerted process.

Moreover, it is of interest to emphasize that the newly formed C−S bond length in **1-S-TS**, **2-S-TS**, and **3-S-TS** is shorter by 13 % – 16 % relative to their value of precursor complex, while the analogous C−S bond in **4-S-TS**, **5-S-TS**, and **6-S-TS** is on average 40 % shorter than that in the corresponding ylide-like complex. These structural features suggest that the barrier is encountered earlier in the reaction of the first three carbenes than in that of the last three. This is definitively reflected in the computed activation energies. As shown in Table 3, the predicted activation barriers for these desulfurization increase in the order: **1-S-TS** (-0.12 kcal mol^{-1}) < **2-S-TS** (-1.7 kcal mol^{-1}) < **3-S-TS** (0.63 kcal mol^{-1}) < **4-S-TS** (2.1 kcal mol^{-1}) < **5-S-TS** (8.2 kcal mol^{-1}) < **6-S-TS** (13 kcal mol^{-1}). Besides, it is evident from Table 3 that all the thiirane desulfurizations are exothermic, and the order of exothermicity follows the same trend as that of the activation energy: cyclobutylidene (**2**, -75 kcal mol^{-1}) < cyclohexylidene (**3**, -73 kcal mol^{-1}) < dimethylcarbene (**1**, -72 kcal mol^{-1}) < phenylchlorocarbene (**4**, -58 kcal mol^{-1}) < methoxyphenylcarbene (**5**, -55 kcal mol^{-1}) < dimethoxycarbene (**6**, -40 kcal mol^{-1}). Consequently, the theoretical findings suggest that the desulfurization of thiirane by alkyl-substituted carbenes is much more favorable both from a kinetic and a thermodynamical viewpoint than by π-donor-substituted carbenes. Again, our results find excellent support in some experiments by Lusztyk, Warkentin, and co-workers.[7]

Comparison with oxirane deoxygenation and thiirane desulfurization

A comparison of the oxirane deoxygenation with the thiirane desulfurization, reveals the following similarities and differences that are worth mentioning. As for the similarities, our model calculations strongly indicate that heteroatom transfer from oxiranes and thiiranes should occur via a ylide-like (two-center) transition state rather than through a persistent ylide intermediate which then fragments. Moreover, regardless of the abstraction reactions applied, our theoretical investigations suggest that the formation of a complex between reactants is highly unlikely to be detected by experiments. Additionally, these abstraction reactions may take place in a concerted fashion, with partial breaking of the two X−C (X = S and O) bonds in the single transition state. It is therefore predicted that these abstractions are highly stereospecific and that the relative configuration of substituent groups is retained completely in the olefins.

While the similarities between the two abstraction reactions for each carbene system are remarkable, the differences between them are more significant. Some points of interest pertinent to the results of the calculations follow:

1) The sulfur ylide-like intermediates have a long-range minimum corresponding to a loosely bound complex between carbene and thiirane, whereas oxygen ylide-like intermediates are more tightly bound in the sense of exhibiting a shorter forming C − O bond length. That is to say, overall, the carbene appears to be bound slightly more weakly in the thiirane ylide-like complex than in the oxirane ones.

2) As discussed earlier, oxirane undergoes concerted deoxygenation by reaction with carbenes via an asynchronous transition state. In contrast, thiirane desulfurization reactions are predicted to be concerted, but more synchronous, via a transition structure with two more-or-less equal breaking bonds.

3) For a given carbene species, the activation barrier for the thiirane desulfurization is smaller than that for the oxirane analogue; this indicates that the former is kinetically more favorable than the latter. This conclusion is in line with experimental observations. It has been reported that, providing reaction conditions remain the same, the desulfurization reactions are generally more efficient than the deoxygenation ones.[7]

4) It is generally found that while both deoxygenation and desulfurization are facile processes, the deoxygenation reaction is more exothermic. Thus, the production of carbonyl compounds is clearly more thermodynamically favorable than that of thiocarbonyl molecules.

In brief, considering both the activation barrier and exothermicity based on the model calculations presented here, we conclude that the resulting carbenic reactivity orders are as follows: cyclobutylidene > dimethylcarbene ≈ cyclohexylidene > phenylchlorocarbene > methoxyphenylcarbene ≫ dimethoxycarbene. In other words, electron-donating groups (or electropositive substituents) on the carbene accelerate the abstraction reaction, whereas electron-withdrawing groups (or π-donor substituents) on the carbene retard the reaction.
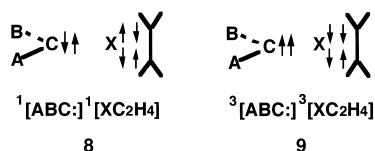
The configuration-mixing model

Although theoretical analysis based on Moss' carbene philicity scale has been used to predict the reactivities of carbene intermediates,[7, 29] we believe that a somewhat different approach and some new aspects emphasized here may supplement their results. According to our theoretical analysis, it was found that all our computational results can be rationalized on the basis of a configuration-mixing (CM) model, which was developed by Pross and Shaik.[20, 31, 32] In this section we show how concepts deduced from the CM model can be used to predict the relative reactivity of reactants.
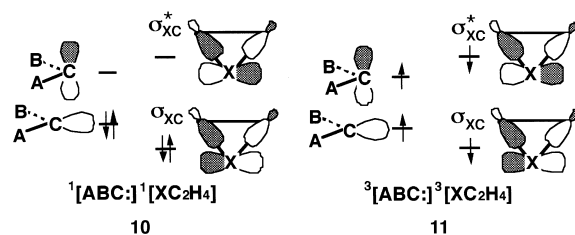
Although many electron configurations of the species involved in the abstraction reaction contribute to the precise form of the energy surface,[31] there are only two predominant configurations that contribute significantly to the total wavefunction Ψ and, in turn, to the potential-energy surface. One is the reactant ground-state configuration that ends up as an excited configuration in the product region. The other is the excited configuration of the reactants that correlates with the ground state of the products.

The key valence bond (VB) configurations for heteroatom-transfer reaction (**8** and **9**) are illustrated in Scheme 2, while the key molecular orbital (MO) configurations (**10** and **11**) are
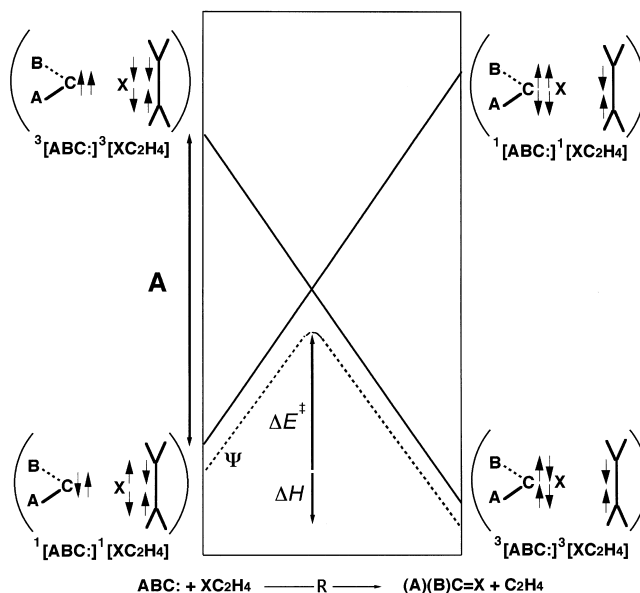

Scheme 3.

Figure 7. The energy diagram for an abstraction reaction showing the formation of a potential-energy curve (Ψ) by mixing two configurations: the reactant configuration and the product configuration. The reactants are separated by an energy gap A. Configuration-mixing near the crossing point causes an "avoided" crossing (dotted line).

Scheme 2.

illustrated in Scheme 3.[33] The VB configuration **8**, labelled ^{1}[ABC:]^1[XC$_2$H$_4$], is termed the *reactant configuration* because this configuration is a good descriptor of the reactants; the two electrons on the ABC: moiety are spin-paired to form the lone pair, while the two electrons on the X heteroatom are spin-paired with the ethylene moiety to form two X–C σ bonds. On the other hand, configuration **9** is the VB *product configuration*. It might initially appear strange that triplet pairs are incorporated into the description of a singlet carbene-abstraction reaction. In reality, however, there is no actual spin change here because, despite the fact that ^{3}[ABC:]^3[XC$_2$H$_4$] appears to contain two triplet pairs, the overall spin state of ^{3}[ABC:]^3[XC$_2$H$_4$] remains a singlet. Moreover, it is a doubly excited configuration only in the reactant geometry. In terms of the product geometry, it is not an excited configuration at all, just the configuration that describes the ground-state abstraction products.[34] The MO representations of VB configurations **8** and **9** are shown in Scheme 3. A schematic energy plot of **8** and **9** (or **10** and **11**) for heteroatom-transfer reaction, as a function of the reaction coordinate (approach of a carbene to the XC$_2$H$_4$ molecule), is illustrated in Figure 7. The ground-state reaction profile, obtained by the mixing of reactant and product configurations, is indicated by the dashed curve and exhibits an activation energy barrier. Thus, it is the avoided crossing of these two configurations that leads to the simplest description

of the ground-state energy profiles for abstraction reactions of the carbene species.[31, 32]

Based on Figure 7 for barrier formation in carbene-abstraction reactions, we are now in a position to provide insight into the parameters that are likely to affect reactivity in this system. The energy of point **9** (left in Figure 7), the anchor point for ^{3}[ABC:]^3[XC$_2$H$_4$] in the reactant geometry, will be governed by the singlet–triplet energy gap for both the carbene and the oxirane (or thiirane), that is, ΔE_{st} ($=E_{triplet} - E_{singlet}$ for ABC:) + $\Delta E_{\sigma\sigma^*}$ ($=E_{triplet} - E_{singlet}$ for XC$_2$H$_4$). In other words, the smaller the $\Delta E_{st} + \Delta E_{\sigma\sigma^*}$ value, the lower the activation barrier and the larger the exothermicity.[31, 32] Bearing the above analysis in mind, we shall explain the origin of the observed trends as shown previously in the following discussion:

a) Why are the alkyl-substituted carbene much more favorable than the π donor-substituted carbenes towards the abstraction reactions with oxirane and thiirane? The driving force for this can be traced to the singlet–triplet energy gap (ΔE_{st}) of the carbene. As analyzed above, if $\Delta E_{\sigma\sigma^*}$ is a constant, the smaller the ΔE_{st} of carbene, the lower the barrier height and the larger the exothermicity, and, in turn, the faster the heteroatom-transfer reaction. Indeed, our theoretical calculations confirm

this prediction. For the B3LYP/6-31G* calculations on the six carbene species studied here, a plot of the activation barrier ($\Delta E^{\neq}$) and the reaction enthalpy (ΔH) versus ΔE_{st} for the oxirane deoxygenation is given in Figure 8: the best fit is

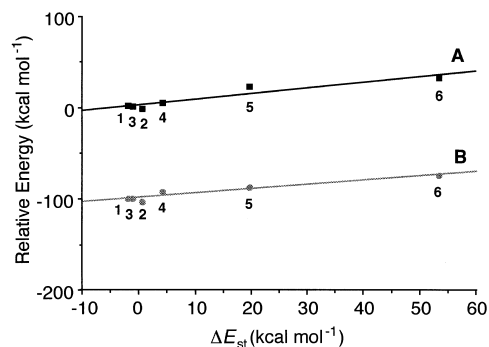Figure 8. ΔE_{st} ($= E_{triplet} - E_{singlet}$) for carbenes **1–6** versus the activation energy and reaction enthalpy for the deoxygenation of oxirane. The linear regression equation is A) $\Delta E^{\neq} = 0.625\Delta E_{st} + 4.00$ and B) $\Delta H = 0.486\Delta E_{st} - 97.7$ with correlation coefficients $r^2 = 0.94$ and $r^2 = 0.94$, respectively. All values were calculated at the B3LYP/6-31G* level, see text.

$\Delta E^{\neq} = 0.625\Delta E_{st} + 4.00$ ($r^2 = 0.936$; $r =$ correlation coefficient) and $\Delta H = 0.486\Delta E_{st} - 97.7$ ($r^2 = 0.944$), respectively. Likewise, the linear correlation between ΔE_{st} and $\Delta E^{\neq}$ as well as ΔH for thiirane desulfurization, also obtained at the same level of theory, are $\Delta E^{\neq} = 0.248\Delta E_{st} + 0.288$ ($r^2 = 0.944$) and $\Delta H = 0.578\Delta E_{st} - 69.3$ ($r^2 = 0.939$), respectively.

Furthermore, since two new bonds have to be formed between the carbene carbon and the heteroatom during the abstraction reaction, the "bond-prepared" carbene state must have at least two open shells, and the lowest state of this type is the triplet state. Accordingly, from the valence-bond point of view, the bonding in the product can be recognized as bonds formed between a triplet carbene state and a triplet heteroatom (overall singlet). This is similar to considering the bonds in a carbon monoxide molecule as being formed between a triplet carbon atom and a triplet oxygen atom.[35] Therefore, if a reactant carbene has a singlet ground state with a low-lying triplet state (and vice versa), it will readily undergo single-step bond abstractions due to involvement of the triplet state in the reaction (remember that the whole abstraction reaction still proceeds on the singlet surface). As noted in the previous section, alkyl substituents lead to a lowering in the energy of the triplet state as relative to that of the singlet state in the carbene species; this results in a smaller singlet–triplet splitting ΔE_{st} ($= E_{triplet} - E_{singlet}$). For example, the B3LYP calculations result in a ΔE_{st} for carbenes **1–3** of -1.9, 0.60, and -1.0 kcal mol^{-1}, respectively. A consequence of the near degeneracy of these two states is their rapid equilibration.[36] Thus, the chemical properties expressed by such carbenes are characteristic of both a singlet and triplet carbene. It is therefore anticipated that a carbene species with the electron-donating substituents (such as the alkyl groups) would lead to a smaller ΔE_{st} and, in turn, allow a more facile heteroatom-transfer reaction.

On the other hand, if the magnitude of the carbene energy gap (ΔE_{st}) separating the triplet from the singlet ground state

is too large to permit participation of its triplet in the reaction, then this would retard the heteroatom-transfer reaction. As mentioned earlier, for the Cl and OCH$_3$ substituents, the singlet–triplet energy gap increases as more potent electron-withdrawing groups are attached to the carbene. This observation can be explained simply as a result of greater stabilization of the singlet than of the triplet by π-donor substituents. For instance, our results show that ΔE_{st} of carbenes **4–6** are 4.3, 19, and 54 kcal mol^{-1}, respectively. These gaps are too large to be overcome within the lifetime of the singlet carbene and thus the three carbenes behave as classical singlet carbenes. It is therefore predicted that by adding π-donor substituents (or electron-withdrawing substituents) such as the Cl and OCH$_3$, the stability of the singlet carbene increases (and thus leads to a larger ΔE_{st}). Consequently, its reactivity toward the abstraction reaction decreases.

b) For a given carbene species, why are the activation barriers for thiirane desulfurization lower than those for oxirane deoxygenation? The reason for this may be traced to $\Delta E_{\sigma\sigma^*}$, which can be evaluated to a good approximation from the energies of the vertical HOMO-1 (the bonding X$-$C σ orbital of XC$_2$H$_4$) $\rightarrow$ LUMO (the antibonding X$-$C σ^* orbital of XC$_2$H$_4$) triplet excitation in oxirane (X $=$ O) and thiirane (X $=$ S).[37] As anticipated by the CM model shown in Figure 7, if ΔE_{st} of carbene is a constant, then a smaller value of $\Delta E_{\sigma\sigma^*}$ leads to a lower barrier height. Our DFT results suggest an decreasing trend in $\Delta E_{\sigma\sigma^*}$ for oxirane (188 kcal mol^{-1}) to thiirane (106 kcal mol^{-1}).[38] This is in good accord with the experimental and theoretical observations as noted earlier, that is, thiirane is more susceptible to a carbene-abstraction reaction than oxirane.

Conclusion

In conclusion, our theoretical attempts to reflect the experimental trend of carbene-abstraction reactions are quite encouraging. In particular, the agreement between DFT and experimental results indicates that the B3LYP/6-31G* method can be an adequate tool to investigate these heteroatom-transfer reactions. Additionally, our work provides strong evidence that the singlet–triplet splitting (ΔE_{st} and $\Delta E_{\sigma\sigma^*}$) can be used as a diagnostic tool to predict the reactivity of the reactants. In consequence, with the above analysis in mind, we are confident in predicting that electron-donating or bulky substituents on the carbene will result in a smaller ΔE_{st} and, in turn, will facilitate the heteroatom-transfer reaction. It should be noted that while both deoxygenation and desulfurization are facile processes, the deoxygenation reaction is more exothermic but less kinetically favored. Besides this, the present model calculations demonstrate that a concerted process that does not involve ylide intermediates should play a dominant role in such abstraction reactions. That is to say, these heteroatom-transfer reactions by carbenes will proceed stereospecifically, leading to an olefin with retained stereochemistry.

Furthermore, as our analysis demonstrates, the CM approach adds additional facets and insights to this relatively poorly understood area of mechanistic study. Although the relative reactivity of various carbenes are determined by the entire potential-energy surfaces, the concepts of the CM model, focusing on the singlet–triplet splitting in the reactants, can allow one to assess quickly the relative reactivity of a variety of carbenes without specific knowledge of the actual energies of the interactions involved. In spite of its simplicity, our approach can provide chemists with important insights into the factors that control the activation energies for heteroatom-transfer reactions and thus permit them to predict the reactivity of some unknown carbenes. The predictions may be useful as a guide to future synthetic efforts and to indicate problems that merit further study by both theory and experiment. It is hoped that our study will stimulate further research into the subject.

Acknowledgements

[1] a) A. Hassner, *Small Rings Heterocycles*, Part III, Wiley, New York, **1985**; b) H. O. House, *Modern Synthetic Reactions*, 2nd ed., Benjamin, Menlo Park, CA, **1972**, Chapters 5 and 7; c) H. Suzuki, T. Fuchita, A. Iwasa, T. Mishina, *Synthesis* **1978**, 905.

[2] a) S. C. Wofsy, J. A. Logan, *Nature* **1986**, *321*, 755; b) R. N. Baruah, R. P. Sharma, J. N. Baruah, *Chem. Ind.* **1983**, 524.

[3] a) S. Togashi, J. G. Fulcher, B. R. Cho, M. Hasegawa, J. A. Gladysz, *J. Org. Chem.* **1980**, *45*, 3044; b) M. Berry, S. G. Davies, M. L. H. Green, *J. Chem. Soc. Chem. Commun.* **1978**, 99; c) K. B. Sharpless, M. A. Umbreit, M. T. Nieh, T. C. Flood, *J. Am. Chem. Soc.* **1972**, *94*, 6538; d) E. E. van Tamelen, J. A. Gladysz, *J. Am. Chem. Soc.* **1974**, 96, 5290; e) H. Ledon, D. Des Roches, *Tetrahedron Lett.* **1977**, 4155.

[4] a) J. E. McMurry, M. G Silvestri, M. P. Fleming, T. Hoz, M. W. Grayston, *J. Org. Chem.* **1978**, *43*, 3249; b) J. E. McMurry, M. P. Fleming, K. L. Kees, L. R. Krepski, *J. Org. Chem.* **1978**, *43*, 3255.

[5] a) A. Hassner, *Small Rings Heterocycles, Part I*, Wiley, New York, **1983**; b) E. Block, *J. Chem. Ed.* **1971**, *48*, 814; c) I. Fleming, *Chem. Ind.* **1975**, 449; d) A. H. Davidson, P. K. G. Hodgson, D. Howells, S. Warren, *Chem. Ind.* **1975**, 455; e) F. Bernardi, I. G. Csizmadia, A. Mangini, *Organic Sulfur Chemistry*, Elsevier, Amsterdam, **1985**; f) L. I. Belen'kii, *Chemistry of Organosulfur Compounds*, Ellis Horwood, New York, **1990**.

[6] a) D. Crich, L. Quintero, *Chem. Rev.* **1989**, *89*, 1414; b) C. P., Jasperse D. P. Curran, T. L. Fevig, *Chem. Rev.* **1991**, *91*, 1237; c) P. Page, *Organosulfur Chemistry*, Academic Press, New York, **1995**.

[7] J. P. Pezacki, P. D. Wood, T. A. Gadosy, J. Lusztyk, J. Warkentin, *J. Am. Chem. Soc.* **1998**, *120*, 8681.

[8] a) G. Wittig, M. Schlosser, *Tetrahedron* **1962**, *18*, 1026; b) H. Nozaki, H. Takaya, R. Noyori, *Tetrahedron Lett.* **1965**, 2563; c) H. Nozaki, H. Takaya, R. Noyori, *Tetrahedron* **1966**, *22*, 3393; d) M. G. Martin, B. Ganem, *Tetrahedron Lett.* **1984**, *25*, 251; e) C. J. Shields, G. B. Schuster, *Tetrahedron Lett.* **1987**, *28*, 853.

[9] M.-D. Su, S.-Y. Chu, *Chem. Phys. Lett.* **2000**, in press.

[10] a) A. D. Becke, *Phys. Rev. A* **1988**, *38*, 3098; b) C. Lee, W. Yang, R. G. Parr, *Phys. Rev. B* **1988**, *37*, 785.

[11] A. D. Becke, *J. Chem. Phys.* **1993**, *98*, 5648.

[12] a) P. von R. Schleyer, N. L. Allinger, T. Clark, J. Gasteiger, P. A. Kollman, H. F. Schaefer III, P. R. Schreiner, *Encyclopedia of Computational Chemistry, Vol. 3*, Wiley, New York, **1998**; b) S. Jursic, *J. Mol. Struct.* **1997**, *401*, 45.

[13] T. Clark, J. Chandrasekhari, G. W. Spitznagel, P. von R. Schleyer, *J. Comput. Chem.* **1983**, *4*, 294.

[14] M. J. Frisch, G. W. Trucks, H. B. Schlegel, P. M. W. Gill, B. G. Johnson, M. A. Robb, J. R. Cheeseman, T. Keith, G. A. Peterson, J. A. Montgomery, K. Raghavachari, M. A. Al-Laham, V. G. Zakrzewski, J. V. Ortiz, J. B. Foresman, J. Cioslowski, B. B. Stefanov, A. Nanayakara, M. Challacombe, C. Y. Peng, P. Y. Ayala, W. Chen, M. W. Wong, J. L. Andres, E. S. Replogle, R. Gomperts, R. L. Martin, D. J. Fox, J. S. Binkley, D. J. Defrees, J. Baker, J. P. Stewart, M. Head-Gordon, C. Gonzalez, J. A. Pople, *Gaussian 94*, Gaussian, Pittsburgh PA, **1995**.

[15] M.-D. Su, *J. Phys. Chem.* **1996**, *100*, 4339, and references therein.

[16] However, some of the geometrical conformations of the triplet carbenes are different from those of the singlet carbenes.

[17] a) C. A. Richards, S.-J. Kim, Y. Yamaguchi, H. F. Schaefer III, *J. Am. Chem. Soc.* **1995**, *117*, 10104; b) S. Matzinger, M. P. Fuscher, *J. Phys. Chem.* **1995**, *99*, 10747.

[18] a) R. Hoffmann, G. D. Zeise, G. W. Van Dine, *J. Am. Chem. Soc.* **1968**, *90*, 1485; b) K. W. Field, G. B. Schuster, *J. Org. Chem.* **1988**, *53*, 4000.

[19] N. C. Baird, K. F. Taylor, *J. Am. Chem. Soc.* **1978**, *100*, 1333.

[20] M.-D. Su, S.-Y. Chu, *Chem. Phys. Lett.* **1999**, *308*, 283.

[21] P. H. Mueller, N. G. Rondan, K. N. Houk, J. F. Harrison, D. Hooper, B. H. Willen, J. F. Leibman, *J. Am. Chem. Soc.* **1981**, *103*, 5049.

[22] E. A. Carter, W. A. Goddard III, *J. Chem. Phys.* **1988**, *88*, 1752.

[23] However, Moss and co-workers predicted that dimethoxycarbene has a singlet ground state with a large ΔE_{st} of 76 kcal mol^{-1}, see: R. A. Moss, M. Wlostowski, S. Shen, K. Krogh-Jespersen, A. Matro, *J. Am. Chem. Soc.* **1988**, *110*, 4443.

[24] Our DFT results are in good agreement with the previous work, in which the most stable conformer of $C(C_6H_5)(OCH_3)$ was calculated to be the *trans* species; see: R. A. Moss, S. Shen, L. M. Hadel, G. Kmiecik-Lawrynowicz, J. Wlostowsks, K. Krogh-Jespersen, *J. Am. Chem. Soc.* **1987**, *109*, 4341.

[25] a) C. Hirose, *Bull. Chem. Soc. Jpn.* **1974**, *47*, 1311; b) K. Okiye, C. Hirose, D. G. Lister, J. Sheridan, *Chem. Phys. Lett.* **1974**, *24*, 111.

[26] D. Kovacs, M.-S. Lee, D. Olson, J. E. Jackson, *J. Am. Chem. Soc.*, **1996**, *118*, 8144, and references therein.

[27] a) M.-D. Su, *Chem. Phys. Lett.* **1995**, *237*, 317; b) M.-D. Su, *J. Org. Chem.* **1995**, *60*, 6621; c) M.-D. Su, *J. Phys. Chem.* **1996**, *100*, 4339; c) M.-D. Su, *Chem. Phys.* **1996**, *205*, 277; e) M.-D. Su, *J. Org. Chem.* **1996**, *61*, 3080; f) M.-D. Su, *Tetrahedron*, **1995**, *51*, 5871; g) M.-D. Su, *Tetrahedron*, **1995**, *51*, 12109.

[28] a) N. S. Isaacs, *Physical Organic Chemistry*, Wiley, New York, **1995**, pp. 199; b) W. Schoeller, R. Schneider, *Chem. Ber* **1997**, *130*, 1013.

[29] a) R. A. Moss, *Acc. Chem. Res.* **1980**, *13*, 58; b) R. A. Moss, *Acc. Chem. Res.* **1989**, *22*, 15.

[30] G. S. Hammond, *J. Am. Chem. Soc.* **1954**, *77*, 334.

[31] a) S. Shaik, H. B. Schlegel, S. Wolfe, *Theoretical Aspects of Physical Organic Chemistry*, Wiley, New York, **1992**; b) A. Pross, *Theoretical and Physical principles of Organic Reactivity*, Wiley, New York, **1995**.

[32] a) R. D. Bach, M.-D. Su, E. Aldabagh, J. L. Andres, H. B. Schlegel, *J. Am. Chem. Soc.* **1993**, *115*, 10237; b) M.-D. Su, *Inorg. Chem.* **1995**, *34*, 3829.

[33] W. L. Jorgensen, L. Salem, *The Organic Chemist's Book of Orbitals*, Academic Press, New York, **1973**.

[34] A. Pross, R. A. Moss, *Tetrahedron Lett.* **1990**, *31*, 4553.

[35] M. Driess, H. Grutzmacher, *Angew. Chem.* **1996**, *108*, 900; M. Driess, H. Grutzmacher, *Angew. Chem. Int. Ed. Engl.* **1996**, *35*, 828.

[36] a) S. C. Lapin, G. B. Schuster, *J. Am. Chem. Soc.* **1985**, *107*, 4243; b) Y.-Z. Li, G. B. Schuster, *J. Org. Chem.* **1988**, *53*, 1273.

[37] The $\Delta E_{\sigma\sigma^*}$ was used in which the triplet state was calculated at B3LYP/6-31G* by using the singlet geometry of the same level; for details see ref. [38]. For pictorial orbitals of oxirane see ref. [33], p. 159.

[38] M.-D. Su, S.-Y. Chu, *Eur. J. Chem.* **1999**, *5*, 198.